JOC The Journal of Organic Chemistry

Article

pubs.acs.org/joc

The Anancomeric Character of the Pharmacophore 1,3,4-Thiadiazoline Framework in Chiral Spiro-Cyclohexyl Derivatives: Effects on Stereochemistry and Spiro-Junction Lability. Thermodynamic Aspects

Sergio Menta,[†] Simone Carradori,[‡] Daniela Secci,[†] Cristina Faggi,[§] Luisa Mannina,[†] Roberto Cirilli,*[,∥] and Marco Pierini*[,†]

[†]Dipartimento di Chimica e Tecnologie del Farmaco, Sapienza Università di Roma, Piazzale Aldo Moro 5, 00185 Rome, Italy

[‡]Department of Pharmacy, "G. D'Annunzio" University of Chieti-Pescara, Via dei Vestini 31, 66100 Chieti, Italy

[§]Dipartimento di Chimica, Università degli studi di Firenze, Via della Lastruccia 13, 50019 Sesto Fiorentino, Florence, Italy

[∥]Dipartimento del Farmaco, Istituto Superiore di Sanità, Viale Regina Elena, 299, 00161 Rome, Italy

Supporting Information

ABSTRACT: Three new and easily accessible chiral compounds, containing the pharmacophore 1,3,4-thiadiazoline nucleus joined by a spiro center to a monoalkyl (methyl or *t*-butyl) substituted cyclohexyl fragment, have been synthesized and fully characterized from the structural and stereochemical point of view. The formation of a spiro-cyclohexyl-thiadiazoline system (sCT) offered the rare opportunity to generate at room temperature both anancomeric structures, displaying alkyl groups bound to the cyclohexyl ring in equatorial position, and other quite stable stereoisomers in which the same alkyl moieties are, instead, inserted in axial position, even for the extreme case represented by the really bulky *t*-butyl group. DFT calculations led to a clear rationalization of such stereochemical behaviors, pointing out that in all cases they arise from the unexpected strong anancomeric character possessed by the sCT framework in its 4-acetyl substituted version. In consideration of the large number of substances in which the 1,3,4-thiadiazoline heterocycle has been found as the active pharmacophore, the results discussed in this work may provide solid bases to allow a rational design of new chiral bioactive spiro-thiadiazolines characterized by well-defined stereochemical structures and single anancomeric geometries.

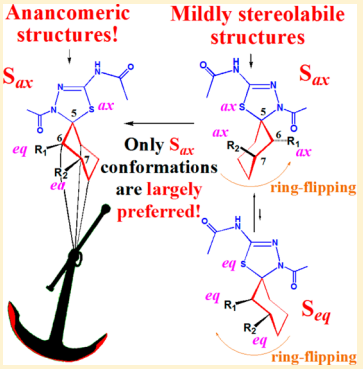

INTRODUCTION

As it is known, spiro structures are constituted by a couple of rings connected through just one common sp^3 hybridized atom, called "spiro atom" (frequently a quaternary "spiro carbon atom"). Due to the tetrahedral nature of the spiro atom, the two rings are not coplanar but twisted almost perpendicularly to each other. These particular arrangements, which are carriers of strong steric constraints, make the construction of all-carbon quaternary centers a formidable challenge for synthetic organic chemists and may markedly characterize the biological activity of synthetic and natural substances that include them in their structure.[1−6]

Nevertheless, literature review reveals that the incorporation of heterocyclic scaffolds into spiro structures attracts considerable attention in synthetic and medicinal chemistry. Among these, the 1,3,4-thiadiazole ring, a five-membered heterocycle, in its original or reduced forms, has been found in molecules endowed with a wide spectrum of pharmacological activities (e.g., antimicrobial, fungicidal, anticancer, analgesic, and anti-inflammatory activity, etc.) probably by virtue of the N═C−S (or its reduced) moiety. Accordingly, this peculiar structural framework has been observed in a variety of natural products and has also been the subject of several syntheses and methodological studies.[7−9] Many drugs containing the thiadiazole nucleus are available on the market, such as acetazolamide, methazolamide, and sulfamethazole. Keeping in mind that the design of new substances based on privileged scaffolds is one of the successful strategies in drug discovery, the recourse to spiro-thiadiazoline structures could be a promising "hybrid pharmacophore" approach to the development of new pharmacological agents.

Starting from this premise, we designed and synthesized a small series of chiral spiro compounds containing the 1,3,4-thiadiazoline nucleus joined, by spiro center, to a cyclohexyl fragment monoalkyl substituted: *N*-(4-acetyl-6- or 7-alkyl-1-thia-3,4-diazaspiro[4.5]dec-2-en-2-yl)-acetamides obtained starting from 2-methylcyclohexanone (compound **1**), 2-*t*-butylcyclohexanone (compound **2**), and 3-methylcyclohexanone (compound **3**, Scheme 1). This choice was based on the consideration that:

Received: July 15, 2015

DOI: 10.1021/acs.joc.5b01635
J. Org. Chem. XXXX, XXX, XXX−XXX

Scheme 1. Series of Spiro Compounds Considered in the Present Work, Each of Which Admitting the Existence of Four Stereoisomers

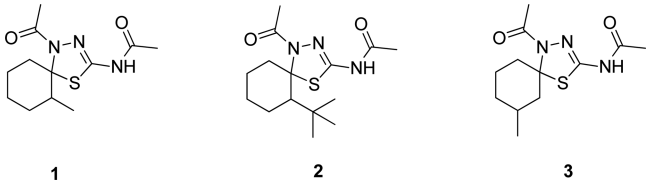

1 2 3

(i) compounds **1**−**3** are easily accessible using cheap reagents;
(ii) in analogy with recent and relevant findings, the three-dimensional structure of these chemotypes could be correlated with stereospecificity to their potential biological activity;[10]
(iii) the C-6 or C-7 substitution on the cyclohexyl fragment offers the possibility to investigate the role played by steric effects rising from the chosen alkyl substituents on the configurational and conformational stability of the structure.

With regard to this latter point, it is well-known as the presence of a *t*-butyl substituent bound to a six-membered carbon ring freezes thermodynamically the chair conformation of the cyclohexyl structure. This is because the axial conformation is largely disadvantaged because of the establishment of strongly destabilizing 1−3 and 1−5 diaxial interactions.[11] Similar effects, of comparable extent, would be advisible and of wide interest if associable to the structural properties of specific pharmacophore frameworks. In the present article, we report about the generation, separation, and characterization of the stereochemistry and thermodynamic stability of both axial and equatorial alkyl-substituted stereoisomers corresponding to the general formulas of the spiro compounds **1**−**3** (Scheme 1). A decisive contribution to the elucidation of the structural aspects concerning the analyzed compounds has been obtained by resorting to X-ray crystallography, as well as by carrying out NMR measurements and a theoretical analysis founded on density functional theory (DFT) calculations.

RESULTS AND DISCUSSION

Synthesis of the Substrates. The synthesis of the spiro compounds **1**−**3** was carried out in two steps. The first synthetic step involves the formation of the spirogenic structure, the thiosemicarbazone of a monosubstituted cyclohexanone, by reaction of the corresponding ketone with thiosemicarbazide in ethanol, using acetic acid as the catalyst. In the second step the cyclization is accomplished by treatment of thiosemicarbazone with acetic anhydride at 90 °C for 1 h. The heterocyclization reaction leads to the *N*-acetylation of the

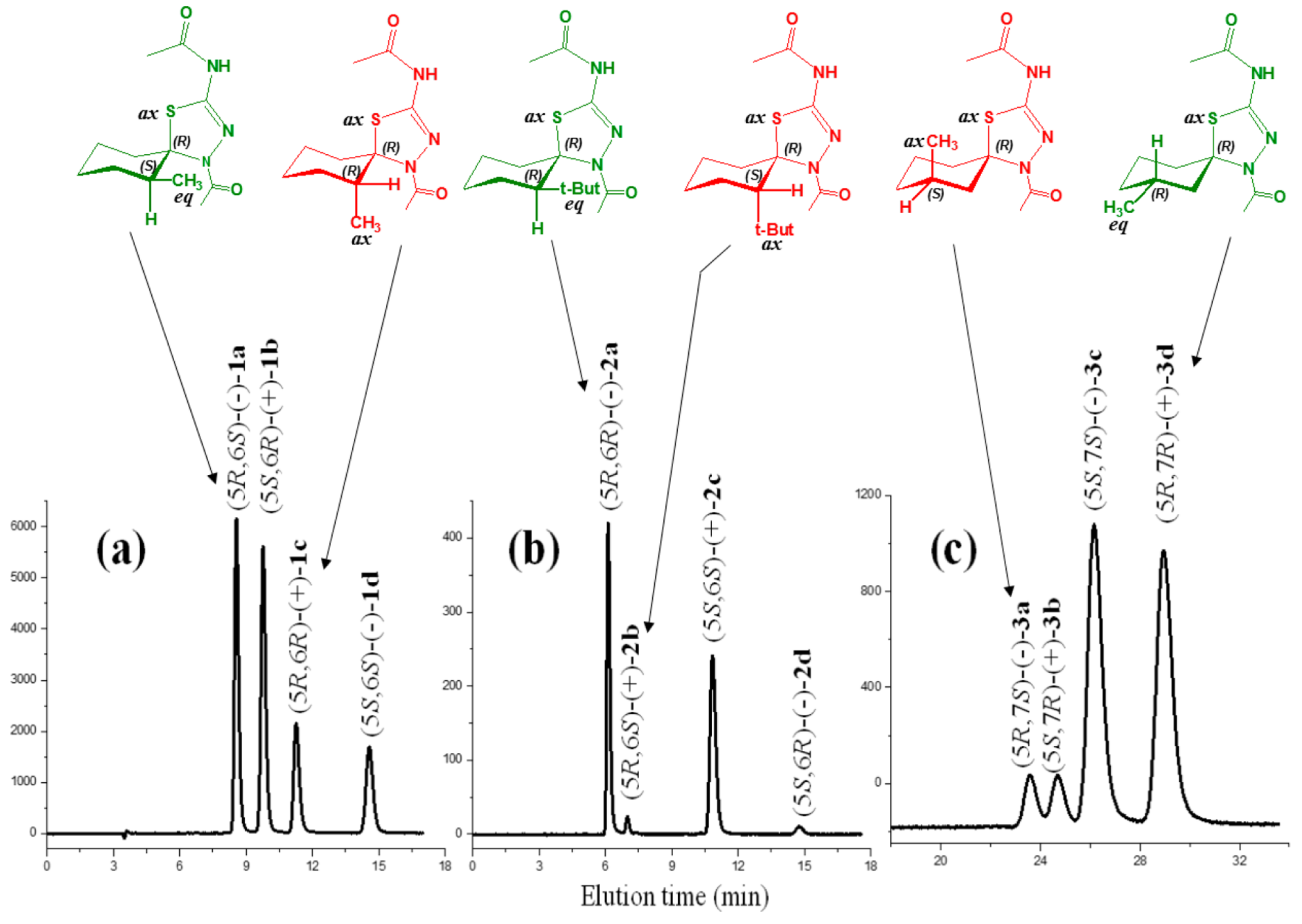

Figure 1. Simultaneous HPLC enantio- and diastereoseparation of **1**−**3** obtained in conditions of kinetic control. Column: Chiralpak IC (250 mm × 4.6 mm i.d.). Eluent: (a) *n*-hexane−ethyl acetate−2-propanol 100:25:1 (v/v/v), (b) *n*-hexane−dichloromethane−2-propanol 10:90:0.5 (v/v/v), and (c) *n*-hexane−ethyl acetate−2-propanol 100:10:1 (v/v/v). Detection: UV at 290 nm. Flow rate: 1.0 mL min^{-1}. Temperature: 25 °C. Diastereomeric ratios: (a) 2.1, (b) 20.6, (c) 7.0.

DOI: 10.1021/acs.joc.5b01635
J. Org. Chem. XXXX, XXX, XXX−XXX

a)

Stereoisomer	$[\alpha]_D^{20}$ (c = 0.1, EtOH)
1a	-8
1b	+8
1c	+343
1d	-340
2a	-30
2b	+258
2c	+29
2d	-257
3a	-52
3b	+53
3c	-11
3d	+12

b)

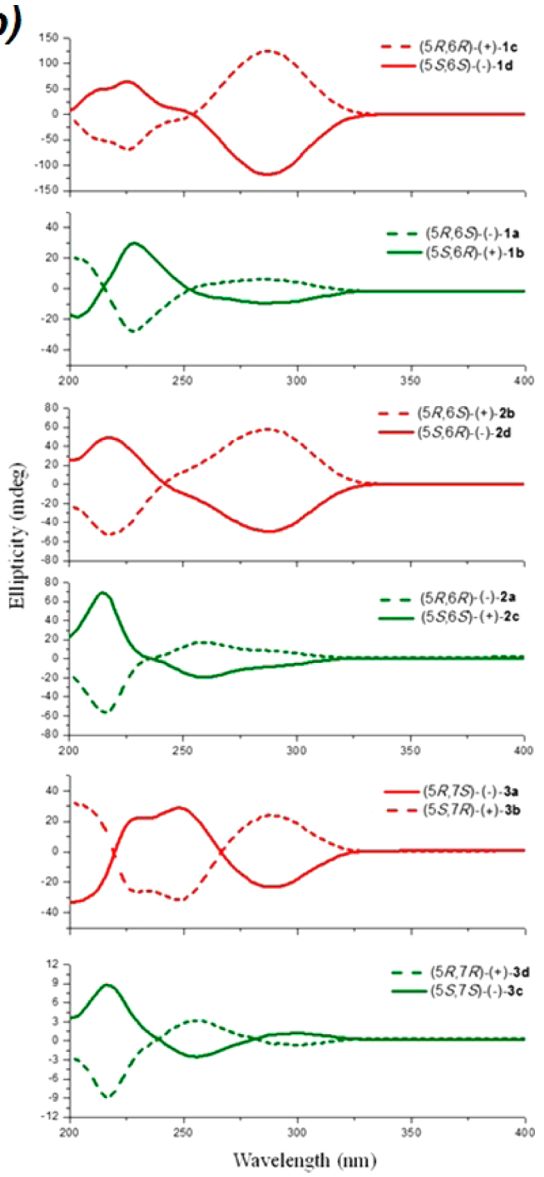

Figure 2. (a) Specific rotations of the stereoisomers of **1**−**3** in ethanol solution. (b) CD spectra of the stereoisomers of **1**−**3** in ethanol solution at 25 °C.

thiosemicarbazone skeleton masked in the 1,3,4-thiadiazoline nucleus of the spiro structure with yields ranging from 71 to 92%, without any distinction about the kind of formed stereoisomers.

Enantioselective and Diastereoselective HPLC. The simultaneous separation of the enantiomers and diastereomers of **1**−**3**, obtained through reactions carried out under kinetic control in order to increase the relative yield of the less stable stereoisomers that are formed faster, was successfully achieved by HPLC on a polysaccharide-based chiral stationary phase under normal phase conditions. In all cases, at 25 °C the chromatographic profile appeared without typical deformations due to competitive on-column interconversion processes taking place on the time scale of the HPLC elution, and the successful separation into the four stereoisomers was clearly visible (Figure 1). In order to distinguish in each chromatogram the four resolved stereoisomers, at this early stage of the discussion we find it convenient to represent them through short symbols, devoid of any direct information regarding the characteristics of the species (i.e., their stereochemistry or relative stability). Each symbol is constituted by a number, corresponding to the analyzed compound (**1**, **2**, or **3**), followed by a letter (**a**, **b**, **c**, or **d**) which denotes the stereoisomeric elution order.

The couple of peaks of equal area could be attributed to a pair of enantiomers, while the peaks with different area could be attributed to species in diastereomeric relationship. This assignment was confirmed by chiroptical measurements (see Figure 2 and next subsection). The values of the diastereomeric ratios (dr) concerning the products formed in conditions of kinetic control (which were provided by HPLC measurements) turn out to be very different, being increased from 2.1 for the compound **1** to 20.6 and 7.0 for the compounds **2** and **3**, respectively, with percentages of the minoritarian diastereomers corresponding to 32.3, 4.6, and 12.5%. The percentages of the same minoritarian diastereomers measured in conditions of thermodynamic control were instead 0.8, 0.3, and 1.0% (±0.1%), respectively (see Experimental Section).

DOI: 10.1021/acs.joc.5b01635
J. Org. Chem. XXXX, XXX, XXX−XXX

Structural Characterization. Structure and absolute configuration of the stereoisomers **1d**, **2b**, **2c**, and **3c**, and indirectly of their enantiomers **1c**, **2d**, **2a** and **3d**, was unambiguously achieved by single crystal X-ray diffraction. Unfortunately, our attempts to obtain crystals of **1a**, **1b**, **3a**, and **3b** of X-ray quality were unsuccessful. Therefore, the stereochemistry of these four stereoisomers has had to be established as follows:

(i) by circular dichroism correlation, performed comparing CD spectra registered for the couple of enantiomers **1a**/**1b** with those of the couple **2a**/**2c** (Figure 2; about this, it is important to note that, due to the different CIP order of priority that the methyl group has with respect to the *t*-butyl one, configuration 6*R** in compound **1** is structurally equivalent to configuration 6*S** in compound **2**);

(ii) by chemical correlation for the couple of enantiomers **3a**/**3b** (for details see Scheme S1).[12]

On this basis, the resulting correspondence between absolute configuration of the species and their HPLC elution order can be summarized as follows:**1a** = (5*R*,6*S*)-**1**; **1b** = (5*S*,6*R*)-**1**; **1c** = (5*R*,6*R*)-**1**; **1d** = (5*S*,6*S*)-**1**; **2a** = (5*R*,6*R*)-**2**; **2b** = (5*R*,6*S*)-**2**; **2c** = (5*S*,6*S*)-**2**; **2d** = (5*S*,6*R*)-**2**; **3a** = (5*R*,7*S*)-**3**; **3b** = (5*S*,7*R*)-**3**; **3c** = (5*S*,7*S*)-**3**; **3d** = (5*R*,7*R*)-**3**.

As shown in the ORTEP projections reported in Figure 3, their molecular conformations are typical of spiro structures with the two rings almost perpendicular with one another. As a further detail, the examination of the crystal structures has also highlighted the conformational axial/equatorial arrangement that the alkyl substituents assume on the cyclohexyl fragment at the solid state. According to this, it is observed that the methyl or *t*-butyl group in the more stable stereoisomers of **2** and **3**, respectively, is arranged in an equatorial disposition of the chair conformation of the cyclohexyl ring, regardless of the position that it occupies (carbon C-6 or C-7) with respect to the spiro center (carbon C-5, Cspiro). Hereafter, when for a same kind of alkyl substitution **1**, **2**, or **3** it will be appropriate to distinguish between the two possible couples of enantiomers, these will be expressed through the shorter symbols *M*-**x** and *L*-**x**, with the letters *M* and *L* indicating the more and less stable couple of enantiomers, respectively, while **x** the species. Coherently, the species **2a**, **2c**, **3c**, and **3d**, visible in the chromatograms b and c of Figure 1 and quoted in the above sentence, will correspond to the predominant pair of enantiomers *M*-**2** and *M*-**3**, respectively.

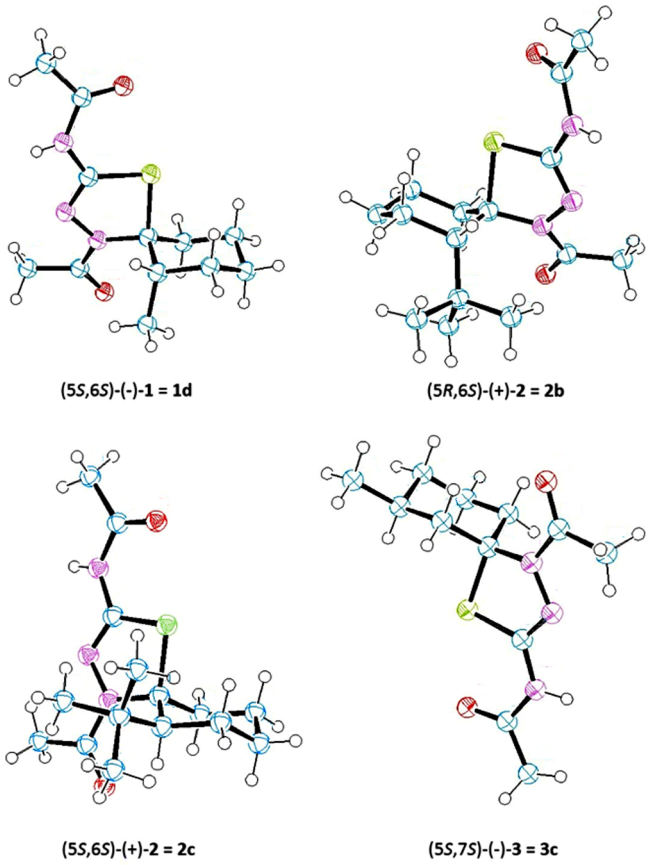

Figure 3. ORTEPs of (5*S*,6*S*)-(−)-**1**, (5*R*,6*S*)-(+)-**2**, (5*S*,6*S*)-(+)-**2**, and (5*S*,7*S*)-(−)-**3**. Ellipsoid contour percent probability: 50%.

Differently from the conformational preferences assumed by the above *M* isomers, in the minoritarian pair of enantiomers of **1** and **2** (i.e., the species *L*-**1** and *L*-**2**), the alkyl group assumes an unusual axial orientation, even in the case of the sterically very demanding *t*-butyl group (compound **2b**). The conformational axial/equatorial arrangement of **1**−**3** on the cyclohexyl fragment, observed by X-ray in the solid state, was experimentally confirmed also in solution ($CDCl_3$ for *M*-**1** and *L*-**1**, while CD_3OD for *M*-**2**, *L*-**2**, *M*-**3**, and *L*-**3**) by ^1H NMR analysis. The assignments were established by suitable analysis of coupling constant values (J_{ab}) relevant to specific protons (see Experimental Section and Supporting Information for details).[13]

Relative Stability of *L* and *M* Diastereomers and Kinetic Aspects of Their Interconversion. The experimental observation that in the course of synthesis of compounds **1**−**3** the less stable diastereomers *L*-**x** are formed faster than their more stable counterparts *M*-**x**, and that, through a suitable choice of operative conditions, it is possible and easy to switch from kinetic to thermodynamic control (allowing in this way the achievement of greater yields of either *L*-**x** or *M*-**x** diastereomers), led us to deepen the knowledge about both the relative stability existing between *L*-**x** and *M*-**x** isomers and the kinetic aspects governing the related isomerization processes. In order to obtain the goal we analyzed the time-dependent decay of the diastereomeric excess of single *L*-**x** stereoisomers isolated as virtually pure or enriched species on a semipreparative scale. More in particular, the spontaneous *L*-**x** → *M*-**x** interconversion, until achieving equilibrium conditions, was monitored as a function of time at 55 °C by classical off-column kinetic determinations in both chloroform ($CHCl_3$) and acetic anhydride (AA, the solvent used in the syntheses of **1**−**3**), using stereoselective HPLC as monitoring tool.[7b,14] The obtained results are collected in Table 1.

As a first observation, inspection of the data reported in Table 1 put in evidence that, with respect to the *L*-**x** isomers, the greater stability possessed by the *M*-**x** species is never lesser than 3 kcal mol^{-1} (compound **3** in AA), reaching for compound **2** the maximum difference of 6.6 kcal mol^{-1} in $CHCl_3$. In fact, these energy gaps lead, at achieved equilibrium, the *M*-**x** structures to largely dominate their diastereomers, from a minimum value of Boltzmann populations of 99.4% to a maximum value virtually indistinguishable from 100%, respectively. This means that under conditions of thermodynamic control, the generation of *M*-**x** structures may be

DOI: 10.1021/acs.joc.5b01635
J. Org. Chem. XXXX, XXX, XXX−XXX

Table 1. Kinetic Results of the Thermal Diastereomerization of 1−3 Monitored by Stereoselective HPLC

no.	solvent	T (°C)	$k_{L\rightarrow M}$[a] (s^{-1})	$k_{M\rightarrow L}$[b] (s^{-1})	$\Delta G^{\ddagger}_{L\rightarrow M}$ (kcal mol^{-1})	$\Delta G^{\ddagger}_{M\rightarrow L}$ (kcal mol^{-1})	$\Delta G^{\circ}_{L\leftrightarrows M}$ (kcal mol^{-1})	$t_{1/2\,L\rightarrow M}$[c]
1	$CHCl_3$	55	8.22×10^{-6}	1.23×10^{-8}	26.90	31.14	−4.24	1 d
	AA	55	2.11×10^{-6}	1.68×10^{-8}	27.79	30.94	−3.15	4 d
2	$CHCl_3$	55	6.68×10^{-5}	2.67×10^{-9}	25.54	32.14	−6.60	174 min
	AA	55	5.06×10^{-5}	1.57×10^{-7}	25.72	29.48	−3.76	248 min
3	$CHCl_3$	55	6.97×10^{-5}	2.80×10^{-7}	25.51	29.11	−3.60	163 min
	AA	55	2.72×10^{-5}	2.58×10^{-7}	26.12	29.16	−3.04	533 min

[a]Diastereomerization rate constants for the $L \rightarrow M$ process. [b]Diastereomerization rate constants for the $M \rightarrow L$ process. [c]$t_{1/2\,L\rightarrow M}$: half-life time of the $L \rightarrow M$ isomerization.

Scheme 2. Structures of Spiro-1,3,4-thiadiazoline-cyclohexyl Derivatives Used as Models[a]

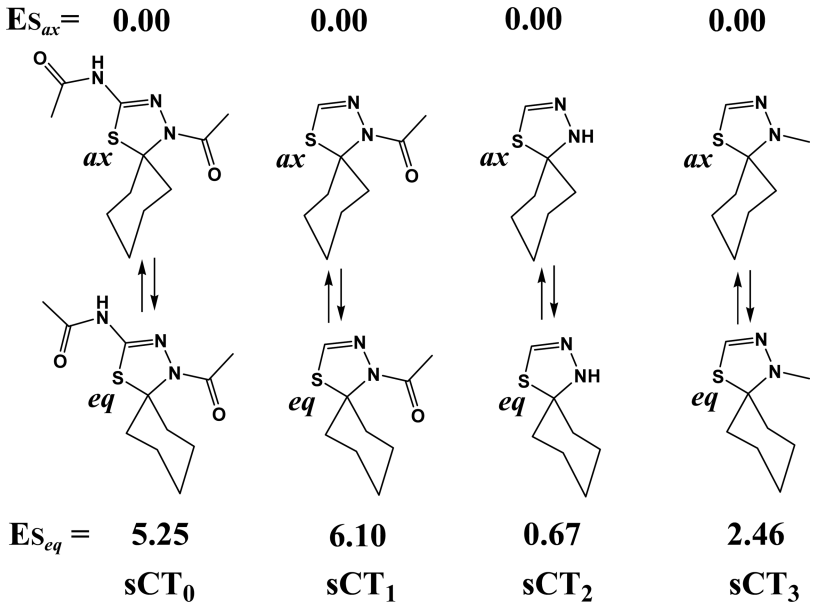

[a]Relative stability energies Es_{eq} and Es_{ax}, computed in chloroform, are reported in kcal mol^{-1}.

considered complete. Second, at the temperature of 55 °C, the $L \rightarrow M$ isomerizations are all characterized by significantly high activation energy barriers, even in the case of the couple of enantiomers *L*-**2** that show the *t*-butyl group in axial disposition. This is stressed by the fact that, at room temperature (and in the hypothesis of a negligible entropy contribution), it is assessed a half-life time of about 7 days (while of about 1 day at the body temperature of 37 °C). Finally, from the data it can also be highlighted that, on increase of solvent polarity, the $L \rightarrow M$ isomerization barriers also increase, although of quite modest amounts.

Generation of Anancomeric Conformations. Besides the particular axial/equatorial arrangement that alkyl groups of **1**−**3** assume on the cyclohexyl fragment, another key property that emerges from inspection of the molecular structures of **1**−**3** in their crystalline state is that the sulfur atom is always found bound in axial to the cyclohexane ring. Therefore, also the quoted stereochemical preferences observed into the crystals must be related to peculiar steric interactions that the substituted 1,3,4-thiadiazoline fragment establishes in answer to its incorporation into the spiro-cyclohexyl system. In order to shed light about such experimental evidence, the structures of compounds **1**−**3**, as well as that of their common spiro-cyclohexyl-4-acetyl-2-acetamido-1,3,4-thiadiazoline framework (hereafter symbolized sCT_0, Scheme 2), that will be used as a reference model, have been modeled by resorting to DFT calculations. Chloroform was the solvent considered in the geometry-optimization procedure. For every compound and each pair of relative configurations (i.e., the homochiral (5*R**,(6 or 7)*R**)-**x** and heterochiral (5*R**,(6 or 7)*S**)-**x** structures, with **x** denoting the species **1**−**3**), also taken into account were the couples of conformational stereoisomers resulting by flip of the cyclohexane ring.

In this way it becomes possible to put in evidence the conformational effects that would arise from the axial (S_{ax}) or equatorial (S_{eq}) disposition of the sulfur atom (i.e., the (5*R**,(6 or 7)*R**)-**x**-S_{ax}, (5*R**,(6 or 7)*R**)-**x**-S_{eq}, (5*R**,(6 or 7)*S**)-**x**-S_{ax}, and (5*R**,(6 or 7)*S**)-**x**-S_{eq} isomers). All the achieved values of absolute and relative energy stability have been collected in Tables 2 (relative values) and S1 (absolute values), respectively.

From their first inspection, it is possible to note that for each of the **1**−**3** compounds the relative energy stabilities experimentally found between the *M* and *L* relevant stereoisomers in chloroform (i.e., the $\Delta G^{\circ CHCl3}_{M-L}$ quantities obtained through the $\Delta G^{\ddagger CHCl3}_{M\rightarrow L} - \Delta G^{\ddagger CHCl3}_{L\rightarrow M}$ differences) have been finely reproduced by calculation. In fact, the experimental $\Delta G^{\circ CHCl3}_{M-L}$ versus computed $\Delta E^{\circ CHCl3}_{M-L}$ values in kcal mol^{-1} are 4.24 against 3.95 for **1**, 6.60 against 7.01 for **2**, and 3.60 against 3.29 for **3** (data from Tables 1 and 2), and this points to a high reliability of the level of theory used in all DFT calculations. Moreover, in all cases, the thermodynamic preference of geometries displaying the sulfur atom in axial position,

DOI: 10.1021/acs.joc.5b01635
J. Org. Chem. XXXX, XXX, XXX−XXX

Table 2. Relative Energy Stabilities in Chloroform of Compounds 1−3 and Model sCT_0

	ORS[a]	configuration[b]	conformation[c]	E (kcal mol^{-1})
sCT_0			S_{ax}	0.00
			S_{eq}	5.25
1	*M*	(5*R**,6*S**)	S_{ax}	0.00
	M	(5*R**,6*S**)	S_{eq}	9.09
	L	(5*R**,6*R**)	S_{ax}	3.95
	L	(5*R**,6*R**)	S_{eq}	5.78
2	*M*	(5*R**,6*R**)	S_{ax}	0.00
	M	(5*R**,6*R**)	S_{eq}	13.29
	L	(5*R**,6*S**)	S_{ax}	7.01
	L	(5*R**,6*S**)	S_{eq}	7.25
3	*M*	(5*R**,7*R**)	S_{ax}	0.00
	M	(5*R**,7*R**)	S_{eq}	7.34
	L	(5*R**,7*S**)	S_{ax}	3.29
	L	(5*R**,7*S**)	S_{eq}	5.10

[a]ORS: order of relative stability between diastereomers. [b]Relative configuration of compounds. [c]Axial or equatorial disposition of sulfur atom on cyclohexane ring.

highlighted by X-ray analysis, has been correctly assessed by theory. This evidence can be rationally justified by considering the computed difference of stability found between the S_{eq} and S_{ax} conformations of the sCT_0 model ($\Delta EsCT_0$-$S_{ax\text{-}eq}$), which amounts to 5.2 kcal mol^{-1}. Such a significant energy gap, arising from less destabilizing S···H and O···H steric interactions in the sCT_0-S_{ax} structure with respect to the flipped conformer sCT_0-S_{eq} (Figure 4), closely resembles the well-known effect

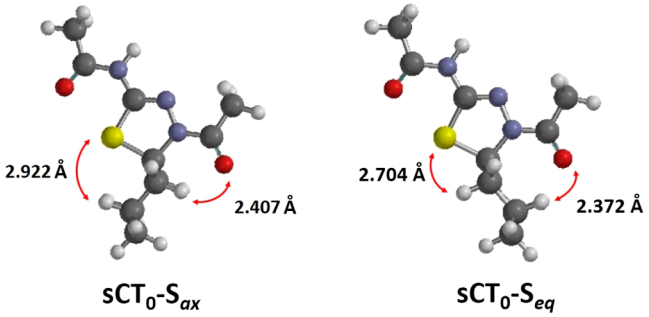

Figure 4. Destabilizing S···H and O···H steric interactions inside the structures of the sCT_0-S_{ax} and sCT_0-S_{eq} conformers.

produced by a *t*-butyl group (***t*Bu**) substituting a hydrogen atom in a cyclohexane ring (**CH**). In this case, indeed, according to literature data, the resulting axial and equatorial conformational stereoisomers (i.e., the **CH-*t*Bu**$_{ax}$ and **CH-*t*Bu**$_{eq}$ species, respectively) differ in energy (ΔE**CH-*t*Bu**$_{ax\text{-}eq}$) by 4.7−5.7 kcal mol^{-1} in favor of the equatorial species.[11,15]

In order to perform the above comparison in consistent operating conditions, we recomputed such a difference by considering in the geometry optimization procedure of **CH-*t*Bu**$_{ax}$ and **CH-*t*Bu**$_{eq}$ the chloroform as the solvent, obtaining 5.5 kcal mol^{-1} as the new value of ΔE**CH-*t*Bu**$_{ax\text{-}eq}$ to be compared with $\Delta EsCT_0$-$S_{ax\text{-}eq}$ (Table 2). Therefore, this result confirms that, similarly to a *t*-butyl group, also the spiro-1,3,4-thiadiazoline moiety, in its 4-acetyl and 2-acetamido substituted version, can act on the cyclohexane ring as an effective "holding framework", leading to the generation of an "anancomeric" structure. About this quite rarely used term, we consider useful to remind that it may be employed to refer to a molecule conformationally "biased" or, in other words, fixed in just one conformation, because of an energy gap from the possible conformational stereoisomers not lower than 2.4 kcal mol^{-1}.[11,15a]

Certainly, this has also a strong and direct reflex on the conformational stability of its possible derivatives, as in fact occurs in the case of compounds **1**−**3**. More in particular, calculations highlighted that the (5*R**,6*S**)-**1**-S_{ax}, (5*R**,6*R**)-**2**-S_{ax}, and (5*R**,7*R**)-**3**-S_{ax} stereoisomers manifest themselves as greatly more stable than their flipped counterparts with S_{eq} and axial alkyl groups (from 7.3 to 13.3 kcal mol^{-1}, Table 2), and therefore endowed with structures strictly anancomeric. Importantly, such species display their alkyl groups always in equatorial disposition, in agreement with the experimental evidence coming from both X-ray and NMR measurements. The highlighted dominant prevalence of **x**-S_{ax} conformers could play a very important role if the species to which it is associated is provided with biological activity (as, indeed, is the case of the considered compounds), being well-known the general relation existing between stereochemistry and bioactivity. Analogously, their related diastereoisomers, always characterized by S_{ax} conformations but alkyl groups in axial disposition, display again a greater stability with respect to their flipped conformers (with S_{eq} and equatorial alkyl groups). Nevertheless, in this case the calculated Boltzmann populations (BP) have been assessed as less than 100% (96% in the case of both (5*R**,6*R**)-**1**-S_{ax} and (5*R**,7*S**)-**3**-S_{ax}, while 60% in that of (5*R**,6*S**)-**2**-S_{ax}). Noteworthy is the fact that, also for these species, the stereochemistry assessed by calculations at the asymmetric atoms 6 or 7 is just that observed by X-ray in the relevant crystals of **1** and **2** and inferred in solution by NMR (Supporting Information). Thus, even though in a not perfectly additive way, the estimated conformational preferences found in **CH-*t*Bu** (i.e., ΔE**CH-*t*Bu**$_{ax\text{-}eq}$ = 5.5 kcal mol^{-1}) and sCT_0 (i.e., $\Delta EsCT_0$-$S_{ax\text{-}eq}$ = −5.2 kcal mol^{-1}) seem roughly to cancel each other within the isomer (5*R**,6*S**)-**2**-S_{ax}, providing the rationale to explain the unusual axial orientation assumed by the *t*-butyl group in this structure.

In consideration of the above interesting findings, we decided to deepen the peculiar behavior of the spiro-1,3,4-thiadiazoline fragment as a function of type of its chemical substitution on the positions 2 and 4. The goal was achieved by extending the DFT calculations to further three simplified models of sCT_0, that is to say, the species denoted as sCT_1, sCT_2, and sCT_3 reported in Scheme 2.

From the obtained results, collected in Table S1 as absolute values and in Scheme 2 as relative data, it is possible to highlight that, starting from the model sCT_0:

(i) the exclusion of the 2-acetamido moiety (sCT_1) leads to a little increase in the difference of energy stability between the related S_{ax} and S_{eq} conformations, which amounts to 0.86 kcal mol^{-1} in favor of the S-axial disposition;

(ii) the contemporary loss of both the 2-acetamido and 4-acetyl groups (sCT_2) leads to a sharp drop in the difference of energy stability existing between the relevant S_{ax} and S_{eq} conformations, with the sCT_2-S_{ax} stereoisomer again more stable than the flipped equatorial one, but this time for only 0.67 kcal mol^{-1};

(iii) the loss of the 2-acetamido moiety and the substitution of the 4-acetyl with a methyl group (sCT_3) leads to a significant reduction in the difference of energy stability

DOI: 10.1021/acs.joc.5b01635
J. Org. Chem. XXXX, XXX, XXX−XXX

between the relevant S_{eq} and S_{ax} conformations, which passes from 5.25 to only 2.46 kcal mol^{-1}.

The whole of these results suggests therefore that specific structural modifications can be rationally pursued in order to modulate in a targeted way the conformational stability of spiro-1,3,4-thiadiazoline-cyclohexyl derivatives. In particular, starting from the essential spiro structure of sCT_2 as the reference, on increasing of the steric hindrance exercisable by a group substituting the nitrogen atom in position 4, also the difference of energy stability between the related S_{ax} and S_{eq} cyclohexyl chair conformations progressively increases in favor of the S_{ax} isomer. As a practical and impressive example of this effect, it may be considered the case of the couple of (5*R**,6*R**)-**2**-S_{ax} enantiomers (i.e., the isomers *M*-**2**-S_{ax}), whose advantage in energy stability with respect to their flipped counterparts (5*R**,6*R**)-**2**-S_{eq} (i.e., the isomers *M*-**2**-S_{eq}) amounts to as much as 13.3 kcal mol^{-1}!

Thus, it appears possible, in principle, to design strictly anancomeric thiadiazaspiro structures in which cyclohexyl substituents endowed with steric hindrance even greater than the *t*-butyl group may be thermodynamically frozen in axial positions.

CONCLUSIONS

The synthesis of chiral spiro-cyclohexyl derivatives of type **1**−**3**, incorporating the pharmacophore 1,3,4-thiadiazoline framework and made different from each other by the presence of an alkyl group of different type or position on the cyclohexane moiety, has been performed in good yields through an easily accessible procedure. By the presence in each compound of two asymmetric centers, the expected generation of four stereoisomers has been confirmed by enantio- and diastereoselective HPLC resolution of the reaction mixture. A complete assignment of the absolute configuration of all the separated species has been accomplished. The couple of less stable enantiomers, *L*-**x**, was found to be generated faster than their diastereomers, so allowing their synthesis as enriched species in the reaction mixture, by adopting conditions of kinetic control. On the contrary, the other couple of more stable enantiomers, *M*-**x**, could be quantitatively obtained under thermodynamic control. The activation energy barrier that opposes the spontaneous *L*-**x** → *M*-**x** diastereomerization has been evaluated by classical off-column kinetic determinations in both acetic anhydride and chloroform. DFT calculations indicated that the greater stability of *M*-**x** geometries with respect to those of *L*-**x** stereoisomers, as well as the capacity of the *L*-**x** isomers to privilege the axial disposition of their alkyl group, can be attributed to the anancomeric character possessed by the common spiro-cyclohexyl-4-acetyl-2-acetamido-1,3,4-thiadiazoline framework. This suggests that, in the future, specific structural modifications can be rationally pursued in order to modulate in a targeted way the conformational stability of spiro-1,3,4-thiadiazoline-cyclohexyl derivatives by inserting a suitable substituent at the N-4 position. In consideration of the pharmacophore activity connected to the 1,3,4-thiadiazoline framework, we believe that all of the findings obtained in the present study may provide solid bases to allow a rational design of new chiral bioactive spirothiadiazolines characterized by well-defined stereochemical structures and single anancomeric geometries. As a further step, conceived in order to complete this study, we have extended the kinetic investigation concerning the *L*-**x** → *M*-**x** diastereomerization. For this purpose we have determined the rate constant of the event in new solvents and temperatures and elucidated, through a theoretical approach, the different mechanisms governing the slow stage of the interconversion for compounds *L*-**1**, *L*-**2**, and *L*-**3**, putting also in evidence the effects played by a change of solvent. The obtained results will be the subject of a new study, focused on mechanistic aspects.

EXPERIMENTAL SECTION

Organic Synthesis. Chemicals, common solvents, and spectral grade solvents were purchased and used without further purification. Melting points (uncorrected) were determined automatically on an FP62 apparatus. ^1H and ^{13}C spectra were recorded at 25 °C on a 600 MHz spectrometer using $CDCl_3$ and CD_3OD as solvents. Chemical shifts are expressed as δ units (parts per millions) relative to the solvent peak. Coupling constants *J* are valued in hertz (Hz). IR spectra were registered on a FT-IR spectrometer. All reactions were monitored by TLC on 0.2 mm thick silica gel plates (60 F_{254}). Plates were visualized by exposing them to ultraviolet (254 and 365 nm) radiation. Silica gel 60 (70−230 mesh) was used for preparative chromatography.

General procedure for the synthesis of 1-(cycloalkyliden)-thiosemicarbazide derivatives: The appropriate ketone (3.4 mmol), with catalytic amounts of acetic acid, was added to a stirring suspension of thiosemicarbazide (0.30 g, 3.4 mmol) in 10 mL of ethanol at 50 °C. After TLC completion of the reaction (12−24 h), the suspension was filtered and the obtained solid washed with petroleum ether, *n*-hexane, and diethyl ether. The crude product was purified by column chromatography (SiO_2, ethyl acetate/*n*-hexane, 3:1).

General procedure for the conventional synthesis of *N*-(4-acetyl-6-/7-alkyl-1-thia-3,4-diazaspiro[4.5]dec-2-en-2-yl)acetamide (**1**−**3**): 1-(2-Cycloalkyliden)thiosemicarbazide (1.5 mmol) was added to acetic anhydride (7.5 mmol) at 90 °C. In order to perform kinetic control, after 1 h the reaction mixture was poured into ice, extracted with $CHCl_3$ (3 × 50 mL), and desiccated over anhydrous sodium sulfate. After evaporation under vacuum, the crude mixture was purified by column chromatography (SiO_2, ethyl acetate/*n*-hexane 4:1). Compound **1**: 92% yield, 0.37 g. Compound **2**: 71% yield, 0.33 g. Compound **3**: 87% yield, 0.35 g.

Information about the differential amounts of diastereomers obtainable under thermodynamic control were achieved by dissolving in acetic anhydride at 95 °C the diastereomeric mixture coming from the reaction conducted under kinetic control, and monitoring over time the conversion of the *L*-**x** stereoisomers in their related *M*-**x** counterparts, until achieving conditions of equilibrium. The final percentages of *L*-**x** and *M*-**x** species were provided by HPLC measurements, with an associate error of 0.1%.

Chiral HPLC. HPLC enantioseparations and diastereoseparations were performed by using the stainless-steel Chiralpak IC[16] (250 mm × 4.6 mm i.d. and 250 mm × 10 mm i.d.) columns. All HPLC and spectral grade solvents were used without further purification. The analytical HPLC apparatus consisted of a pump equipped with a Rheodyne injector, a 20 μL sample loop, a HPLC oven, and a UV/CD detector. For semipreparative separations, a 500 μL sample loop was used.

HRMS Experiments. The considered compounds were dissolved in MeOH ($\sim 10^{-6}$ M) and analyzed with an orbitrap mass spectrometer set as follows: source, ESI (positive); capillary temp, 275 °C; spray voltage, 3.5 kV; capillary voltage 65 V; tube lens, 125 V.

Compound **1a**: $C_{12}H_{20}N_3O_2S$ requires 270.1271 (monoisotopic mass), *m*/*z* found 270.1269 ($[M + H]^+$), accuracy 0.7 ppm; $C_{12}H_{19}N_3O_2SNa$ requires 292.1090 (monoisotopic mass), *m*/*z* found 292.1085 ($[M + Na]^+$), accuracy 1.7 ppm.

Compound **3a**: $C_{12}H_{20}N_3O_2S$ requires 270.1271 (monoisotopic mass), *m*/*z* found 270.1269 ($[M + H]^+$), accuracy 0.7 ppm; $C_{12}H_{19}N_3O_2SNa$ requires 292.1090 (monoisotopic mass), *m*/*z* found 292.1084 ($[M + Na]^+$), accuracy 2.0 ppm.

DOI: 10.1021/acs.joc.5b01635
J. Org. Chem. XXXX, XXX, XXX−XXX

Off-Column Studies. In off-column diastereomerization studies, solutions of stereoisomers of **1**−**3** (concentration about 0.1 mg/mL) were held at a fixed temperature in a closed vessel. The temperature was monitored by a thermostat. Samples were withdrawn at fixed time intervals and analyzed by HPLC on the Chiralpak IC (250 mm × 4.6 mm i.d.) column.

Polarimetry. Specific rotations were measured at 589 nm by a polarimeter equipped with Na/Hg lamps. The volume of the cell was 1 mL, and the optical path was 10 cm. The system was set at a temperature of 20 °C.

Circular Dichroism. The circular dichroism spectra were measured by using a spectropolarimeter. The optical path and temperature were set at 0.1 mm and 25 °C, respectively. The spectra are average computed over three instrumental scans, and the intensities are presented in terms of ellipticity values (mdeg).

Molecular Modeling Calculations. All calculations were performed with the software package SPARTAN 10, v. 1.1.0. Structures of ground states of spirothiadiazoline derivatives **1**−**3**, as well as those of models sCT_0−sCT_3, were modeled in two steps, first performing a SCF optimization at the HF/3-21G level of theory, next refining the obtained geometries through B3LYP/6-31G(d) calculations. In all cases, chloroform was the simulated medium, according to the SM8 solvation model implemented in Spartan. Afterward, in order to take into suitable account nonbonding interactions, all the above generated ground state geometries were also submitted to single point energy calculations performed at the higher level of theory M06-2x/6-31+G(d), the M06-2x method being a meta-hybrid GGA DFT functional known to have a very good response under dispersion forces.[17]

NMR Spectroscopy. Samples *M*-**1** and *L*-**1** were dissolved in $CDCl_3$ (700 μL) whereas samples *M*-**2**, *L*-**2**, *M*-**3**, and *L*-**3** in CD_3OD (700 μL). NMR spectra were recorded at 300 K on a spectrometer operating at 600.13 MHz and equipped with a multinuclear *z*-gradient inverse probe head capable of producing gradients in the *z* direction with a strength of 55 G cm^{-1}. 2D NMR experiments, namely, $^1H-^1H$ COSY and $^1H-^{13}C$ HSQC, have been acquired using a time domain of 1024 data points in the F2 dimension and 512 data points in the F1 dimension, and the recycle delay was 2 s. The HSQC experiments were performed using a coupling constant $^1J_{C-H}$ of 150 Hz. The number of scans has been optimized for obtaining a good signal/noise ratio. ^1H NMR spectra were referenced with respect to the residual proton signal of $CDCl_3$ and CD_3OD at 7.26 and 3.31 ppm, respectively.[18]

M-**1**. ^1H NMR (600 MHz, $CDCl_3$, Me_4Si): δ 0.937 (d, *J* = 6.5 Hz, 3H, eq CH_3-6), 1.072 (dddd, *J* = 13.2 Hz, *J* = 13.1 Hz, *J* = 13.1 Hz, *J* = 3.4 Hz, 1H, ax. CH_2-7), 1.339 (ddddd, *J* = 13.1 Hz, *J* = 13.1 Hz, *J* = 13.1 Hz, *J* = 3.6 Hz, *J* = 3.6 Hz, 1H, ax. CH_2-8), 1.442 (ddddd, *J* = 13.3 Hz, *J* = 13.3 Hz, *J* = 13.3 Hz, *J* = 3.5 Hz, *J* = 3.5 Hz, 1H, ax. CH_2-9), 1.628 (dm, *J* = 13.2 Hz, 1H, eq CH_2-8), 1.686 (dm, *J* = 13.2 Hz, 1H, eq CH_2-7), 1.807 (dm, *J* = 13.2 Hz, 1H, eq CH_2-9), 2.125 (dm, *J* = 13.2 Hz, 1H, eq CH_2-10), 2.174 (s, 3H, CH_3), 2.183 (s, 3H, CH_3), 2.930 (ddd, *J* = 13.2 Hz, *J* = 13.2 Hz, *J* = 4.0 Hz, 1H, ax. CH_2-10), 3.007 (qdd, *J* = 6.5 Hz, *J* = 13.1 Hz, *J* = 3.2 Hz, 1H, ax. CH-6), 8.350 (s, 1H, NH). ^{13}C NMR (150 MHz, $CDCl_3$): δ 16.7 (CH_3-6), 23.6 (CH_3), 24.6 (CH_3), 24.8 (CH_2-9), 25.2 (CH_2-8), 32.9 (CH_2-7), 37.0 (CH-6), 37.4 (CH_2-10), 91.4 (C_{spiro}), 143.2 (S−C═N), 168.3 (CO), 169.7 (CO).

L-**1**. ^1H NMR (600 MHz, $CDCl_3$, Me_4Si): δ 1.100 (d, *J* = 7.0 Hz, 3H, ax. CH_3-6), 1.278 (ddddd, *J* = 13.5 Hz, *J* = 13.5 Hz, *J* = 13.5 Hz, *J* = 3.8 Hz, *J* = 3.8 Hz, 1H, ax. CH_2-9), 1.480 (m, 1H, eq CH_2-8), 1.528 (m, 1H, eq CH_2-7), 1.540 (m, 1H, ax. CH_2-8), 1.957 (dm, *J* = 13.7 Hz, 1H, eq CH_2-9), 2.028 (dddd, *J* = 14.0 Hz, *J* = 14.0 Hz, *J* = 4.3 Hz, *J* = 4.3 Hz, 1H, ax. CH_2-7), 2.135 (dm, *J* = 13.9 Hz, 1H, eq CH_2-10), 2.185 (s, 3H, CH_3), 2.202 (s, 3H, CH_3), 2.300 (m, 1H, eq CH-6), 3.550 (ddd, *J* = 13.5 Hz, *J* = 13.5 Hz, *J* = 4.1 Hz, 1H, ax. CH_2-10), 7.970 (s, 1H, NH). ^{13}C NMR (150 MHz, $CDCl_3$): δ 16.0 (CH_3-6), 19.8 (CH_2-8), 23.7 (CH_3), 24.8 (CH_3), 27.3 (CH_2-9), 29.7 (CH_2-7), 31.8 (CH_2-10), 41.8 (CH-6), 89.5 (C_{spiro}), 146.1 (S−C═N), 167.9 (CO), 170.8 (CO).

M-**2**. ^1H NMR (600 MHz, CD_3OD, Me_4Si): δ 1.012 (s, 9H, eq *t*Bu-6), 1.109 (dddd, *J* = 13.3 Hz, *J* = 13.3 Hz, *J* = 13.3 Hz, *J* = 3.1 Hz, 1H, ax. CH_2-7), 1.293 (ddddd, *J* = 13.2 Hz, *J* = 13.2 Hz, *J* = 13.2 Hz, *J* = 3.6 Hz, *J* = 3.6 Hz, 1H, ax. CH_2-8), 1.551 (ddddd, *J* = 13.5 Hz, *J* = 13.5 Hz, *J* = 13.5 Hz, *J* = 3.9 Hz, *J* = 3.9 Hz, 1H, ax. CH_2-9), 1.740 (dm, *J* = 13.0 Hz, 1H, eq CH_2-8 or eq CH_2-9), 1.760 (dm, *J* = 13.0 Hz, 1H, eq CH_2-8 or eq CH_2-9), 1.912 (dm, *J* = 13.0 Hz, 1H, eq CH_2-10), 2.008 (dm, *J* = 13.5 Hz, 1H, eq CH_2-7), 2.091 (s, 3H, CH_3), 2.113 (s, 3H, CH_3), 2.898 (ddd, *J* = 13.4 Hz, *J* = 13.4 Hz, *J* = 4.1 Hz, 1H, ax. CH_2-10), 2.945 (dd, *J* = 12.4 Hz, *J* = 3.0 Hz, 1H, ax. CH-6). ^{13}C NMR (150 MHz, CD_3OD): δ 22.7 (CH_3), 25.2 (CH_3), 25.2 (CH_2-9), 27.3 (CH_2-8), 29.4 (3 x CH_3), 30.7 (CH_2-7), 35.7 ($C(CH_3)_3$), 41.9 (CH_2-10), 50.1 (CH-6), 88.9 (C_{spiro}), 145.3 (S−C═N), 171.5 (CO), 172.1 (CO).

L-**2**. ^1H NMR (600 MHz, CD_3OD, Me_4Si): δ 1.052 (s, 9H, ax. *t*Bu-6), 1.440 (m, 1H, eq CH_2-9), 1.513 (m, 1H, eq CH_2-8), 1.713 (m, 1H, ax. CH_2-8), 1.780 (m, 1H, eq CH_2-7), 1.854 (m, 1H, ax. CH_2-9), 1.860 (dd, *J* = 8.7 Hz, *J* = 3.7 Hz, 1H, eq CH-6), 2.036 (dm, *J* = 13.6 Hz, 1H, eq CH_2-10), 2.087 (s, 3H, CH_3), 2.155 (s, 3H, CH_3), 2.220 (m, 1H, ax. CH_2-7), 3.278 (ddd, *J* = 13.6 Hz, *J* = 13.0 Hz, *J* = 3.6 Hz, 1H, ax. CH_2-10). From the $^1H-^{13}C$ HSQC experiment (there are five missing signals): ^{13}C NMR (150 MHz, CD_3OD) δ 22.6 (CH_3), 23.4 (CH_2-8), 23.6 (CH_2-9), 24.3 (CH_2-7), 25.3 (CH_3), 30.6 (3 x CH_3), 37.9 (CH_2-10), 56.7 (CH-6).

M-**3**. ^1H NMR (600 MHz, CD_3OD, Me_4Si): δ 0.960 (qd, *J* = 13.1 Hz, *J* = 3.9 Hz, 1H, ax. CH_2-8), 0.961 (d, *J* = 6.5 Hz, 3H, eq CH_3-7), 1.490 (qt, *J* = 13.7 Hz, *J* = 3.5 Hz, 1H, ax. CH_2-9), 1.562 (m, 1H, ax. CH-7), 1.684 (dm, *J* = 13.0 Hz, 1H, eq CH_2-8), 1.842 (dm, *J* = 13.9 Hz, 1H, eq CH_2-9), 1.978 (dm, *J* = 13.0 Hz, 1H, eq CH_2-10), 2.000 (dm, *J* = 12.3 Hz, 1H, eq CH_2-6), 2.077 (s, 3H, CH_3), 2.179 (s, 3H, CH_3), 2.640 (t, *J* = 12.4 Hz, 1H, ax. CH_2-6), 2.843 (td, 1H, ax. CH_2-10). ^{13}C NMR (150 MHz, $CDCl_3$): δ 22.6 (CH_3-7), 22.7 (CH_3), 24.6 (CH_3), 25.3 (CH_2-9), 33.0 (CH-7), 34.5 (CH_2-8), 36.4 (CH_2-10), 45.3 (CH_2-6), 85.8 (C_{spiro}), 145.5 (S−C═N), 171.4 (CO), 171.9 (CO).

L-**3**. ^1H NMR (600 MHz, CD_3OD, Me_4Si): δ 1.098 (d, *J* = 7.5 Hz, 3H, ax. CH_3-7), 1.420 (dm, *J* = 13.0 Hz, 1H, eq CH_2-8), 1.607 (m, 1H, ax. CH_2-8), 1.680 (m, 2H, ax. and eq CH_2-9), 1.920 (dm, *J* = 13.9 Hz, 1H, eq CH_2-6), 1.963 (dm, *J* = 13.2 Hz, 1H, eq CH_2-10), 2.077 (s, 3H, CH_3), 2.187 (s, 3H, CH_3), 2.243 (m, 1H, eq CH-7), 2.772 (dm, *J* = 13.2 Hz, 1H, ax. CH_2-10), 3.395 (dd, *J* = 13.9 Hz, *J* = 5.9 Hz, 1H, ax. CH_2-6). ^{13}C NMR (150 MHz, $CDCl_3$): δ 19.8 (CH_2-9), 20.4 (CH_3-7), 22.7 (CH_3), 25.0 (CH_3), 29.5 (CH-7), 31.2 (CH_2-8), 37.0 (CH_2-10), 41.7 (CH_2-6), 83.5 (C_{spiro}), 146.3 (S−C═N), 171.5 (CO), 172.1 (CO).

X-ray Diffraction Data. Cu Kα radiation (40 mA/−40 kV) was used for cell parameter determination. The integrated intensities, measured using the ω scan mode, were corrected for Lorentz and polarization effects.[19]

Direct methods of SIR2004[20] were used in solving the structures, and they were refined using the full-matrix least-squares on F2 provided by SHELXL97.[21]

Multiscan symmetry-related measurement was used as experimental absorption correction type. The non-hydrogen atoms were refined anisotropically whereas hydrogen atoms were refined as isotropic.

The X-ray CIF files for these structures have been deposited at the Cambridge Crystallographic Data Center and allocated with the deposition numbers CCDC 866489 for **1d**, CCDC 866490 for **3c**, CCDC 1062909 for **2b**, and CCDC 1062910 for **2c**. Copies of the data can be obtained, free of charge, from the Cambridge Crystallographic Data Centre, 12 Union Road, Cambridge, CB2 1EZ U.K., via www.ccdc.cam.ac.uk/data_request/cif.

Details about crystal data for compounds **1d**, **2b**, **2c** and **3c** are given in Supporting Information.

■ ASSOCIATED CONTENT

Supporting Information

The Supporting Information is available free of charge on the ACS Publications website at DOI: 10.1021/acs.joc.5b01635.

DOI: 10.1021/acs.joc.5b01635
J. Org. Chem. XXXX, XXX, XXX−XXX

Experimental and characterization details (PDF)
X-ray crystallogrpahic data (CIF)

AUTHOR INFORMATION

Corresponding Authors

*roberto.cirilli@iss.it
*marco.pierini@uniroma1.it

Author Contributions

Sergio Menta and Simone Carradori contributed equally to this work.

Notes

The authors declare no competing financial interest.

ACKNOWLEDGMENTS

This work was conducted with financial support from the Sapienza University Contract No. C26A143MYA (2014) and MIUR (PRIN 2010-11, prot. 2010N3T9M4).

REFERENCES

(1) Haberhauer, G.; Ernst, S.; Wilch, C. *Chem. - Eur. J.* **2011**, *17*, 8643.
(2) Ito, H.; Abe, T.; Saigo, K. *Angew. Chem., Int. Ed.* **2011**, *50*, 7144.
(3) Alkorta, I.; Elguero, J. *Tetrahedron: Asymmetry* **2010**, *21*, 437.
(4) Singh, G. S.; Desta, Z. Y. *Chem. Rev.* **2012**, *112*, 6104.
(5) Wunsch, B. *Curr. Pharm. Des.* **2012**, *18*, 930.
(6) Zhou, L.; Zhao, J.; Shan, T.; Cai, X.; Peng, Y. *Mini-Rev. Med. Chem.* **2010**, *10*, 977.
(7) (a) Umamatheswari, S.; Balaji, B.; Ramanathan, M.; Kabilan, S. *Bioorg. Med. Chem. Lett.* **2010**, *20*, 6909. (b) Carradori, S.; Cirilli, R.; Dei Cicchi, S.; Ferretti, R.; Menta, S.; Pierini, M.; Secci, D. *J. Chromatogr. A* **2012**, *1269*, 168.
(8) Li, J. J.; Liang, X. M.; Jin, S. H.; Zhang, J. J.; Yuan, H. Z.; Qi, S. H.; Chen, F. H.; Wang, D. Q. *J. Agric. Food Chem.* **2010**, *58*, 2659.
(9) Hafez, H. N.; Hegab, M. I.; Ahmed-Farag, I. S.; el-Gazzar, A. B. *Bioorg. Med. Chem. Lett.* **2008**, *18*, 4538.
(10) Almansour, A. I.; Kumar, R. S.; Beevi, F.; Shirazi, A. N.; Osman, H.; Ismail, R.; Choon, T. S.; Sullivan, B.; McCaffrey, K.; Nahhas, A.; Parang, K.; Ali, M. A. *Molecules* **2014**, *19*, 10033.
(11) (a) Eliel, E.; Wilen, S. H.; Mander, L. N. *Stereochemistry of Organic Compounds*; Wiley & Sons: New York, 1993.
(12) (a) Berova, N.; Di Bari, L.; Pescitelli, G. *Chem. Soc. Rev.* **2007**, *36*, 914. (b) Specht, K. M.; Nam, J.; Ho, D. M.; Berova, N.; Kondru, R. K.; Beratan, D. N.; Wipf, P.; Pascal, R. A., Jr.; Kahne, D. *J. Am. Chem. Soc.* **2001**, *123*, 8961.
(13) Gordon, A. J.; Ford, R. A. *The Chemist's Companion. A handbook of practical data, techniques, and references*; Wiley: New York, 1972.
(14) (a) Ghirga, F.; D'Acquarica, I.; Delle Monache, G.; Mannina, L.; Molinaro, C.; Nevola, L.; Sobolev, A. P.; Pierini, M.; Botta, B. *J. Org. Chem.* **2013**, *78*, 6935. (b) Cirilli, R.; Costi, R.; Di Santo, R.; Gasparrini, F.; La Torre, F.; Pierini, M.; Siani, G. *Chirality* **2009**, *21*, 24. (c) Cirilli, R.; Costi, R.; Di Santo, R.; La Torre, F.; Pierini, M.; Siani, G. *Anal. Chem.* **2009**, *81*, 3560. (d) Siani, G.; Angelini, G.; De Maria, P.; Fontana, A.; Pierini, M. *Org. Biomol. Chem.* **2008**, *6*, 4236. (e) Angelini, G.; De Maria, P.; Fontana, A.; Pierini, M.; Siani, G. *J. Org. Chem.* **2007**, *72*, 4039. (f) Cirilli, R.; Ferretti, R.; La Torre, F.; Secci, D.; Bolasco, A.; Carradori, S.; Pierini, M. *J. Chromatogr. A* **2007**, *1172*, 160. (g) Botta, B.; D'Acquarica, I.; Delle Monache, G.; Nevola, L.; Tullo, D.; Ugozzoli, F.; Pierini, M. *J. Am. Chem. Soc.* **2007**, *129*, 11202. (h) 16) Fontana, A.; De Maria, P.; Pierini, M.; Siani, G.; Cerritelli, S.; Macaluso, G. *J. Phys. Org. Chem.* **2002**, *15*, 247. (i) 12) Fontana, A.; De Maria, P.; Siani, G.; Pierini, M.; Cerritelli, S.; Ballini, R. *Eur. J. Org. Chem.* **2000**, *2000*, 1641. (j) Gasparrini, F.; Misiti, D.; Pierini, M.; Villani, C. *Tetrahedron: Asymmetry* **1997**, *8*, 2069. (k) Wolf, C. *Dynamic Stereochemistry of Chiral Compounds: Principles and Applications*; RSC Publishing: London, 2008. (l) Wolf, C. *Chem. Soc. Rev.* **2005**, *34*, 595−608.
(15) (a) Anteunis, M.; Tavernier, D.; Borremans, F. *Bull. Soc. Chim. Belg.* **1966**, *75*, 396. (b) Pihlaja, K. *J. Chem. Soc., Perkin Trans. 2* **1974**, 890−896. (c) Booth, H.; Everett, J. R. *J. Chem. Soc., Perkin Trans. 2* **1980**, 255−259.
(16) (a) Benincori, T.; Bonometti, V.; Cirilli, R.; Mussini, P. R.; Marchesi, A.; Pierini, M.; Pilati, T.; Rizzo, S.; Sannicolò, F. *Chem. - Eur. J.* **2013**, *19*, 165−181. (b) Gallinella, B.; Bucciarelli, L.; Zanitti, L.; Ferretti, R.; Cirilli, R. *J. Chromatogr. A* **2014**, *1339*, 210−213. (c) Ferretti, R.; Gallinella, B.; La Torre, F.; Zanitti, L.; Turchetto, L.; Mosca, A.; Cirilli, R. *J. Chromatogr. A* **2009**, *1216*, 5385−5390. (d) Zhang, T.; Nguyen, D.; Franco, P.; Isobe, Y.; Michishita, T.; Murakami, T. *J. Pharm. Biomed. Anal.* **2008**, *46*, 882−891.
(17) (a) Tishchenko, O.; Truhlar, D. G. *J. Phys. Chem. Lett.* **2012**, *3*, 2834. (b) Hermans, I.; Jacobs, P.; Peeters, J. *Phys. Chem. Chem. Phys.* **2008**, *10*, 1125. (c) Zhao, Y.; Truhlar, D. G. *Theor. Chem. Acc.* **2008**, *120*, 215. (d) Bernini, R.; Crisante, F.; Gentili, P.; Menta, S.; Morana, F.; Pierini, M. *RSC Adv.* **2014**, *4*, 8183.
(18) Braun, S.; Kalinowski, H.-O.; Berger, S. *150 and more basic NMR experiments: a practical course*; Wiley-VCH: Weinheim, Germany, 1998.
(19) Walker, N.; Stuart, D. *Acta Crystallogr., Sect. A: Found. Crystallogr.* **1983**, *39*, 158−166.
(20) Burla, M. C.; Caliandro, R.; Camalli, M.; Carrozzini, B.; Cascarano, G. L.; De Caro, L.; Giacovazzo, C.; Polidori, G.; Spagna, R. *J. Appl. Crystallogr.* **2005**, *38*, 381.
(21) Sheldrick, G. M. *SHELXL97: Program for Crystal Structure Refinement*; Institut für Anorganische Chemie de Universitat Göttingen: Göttingen, German, 1997.

DOI: 10.1021/acs.joc.5b01635
J. Org. Chem. XXXX, XXX, XXX−XXX